

## **Electronic supplementary information**

### **Hierarchically porous sheath-core graphene-based fiber-shaped supercapacitors with high energy density**

Xianhong Zheng<sup>1,2</sup>, Kun Zhang<sup>\*1,2</sup>, Lan Yao<sup>1,2</sup>, Yiping Qiu<sup>1,2,3</sup>, Shiren Wang<sup>4</sup>

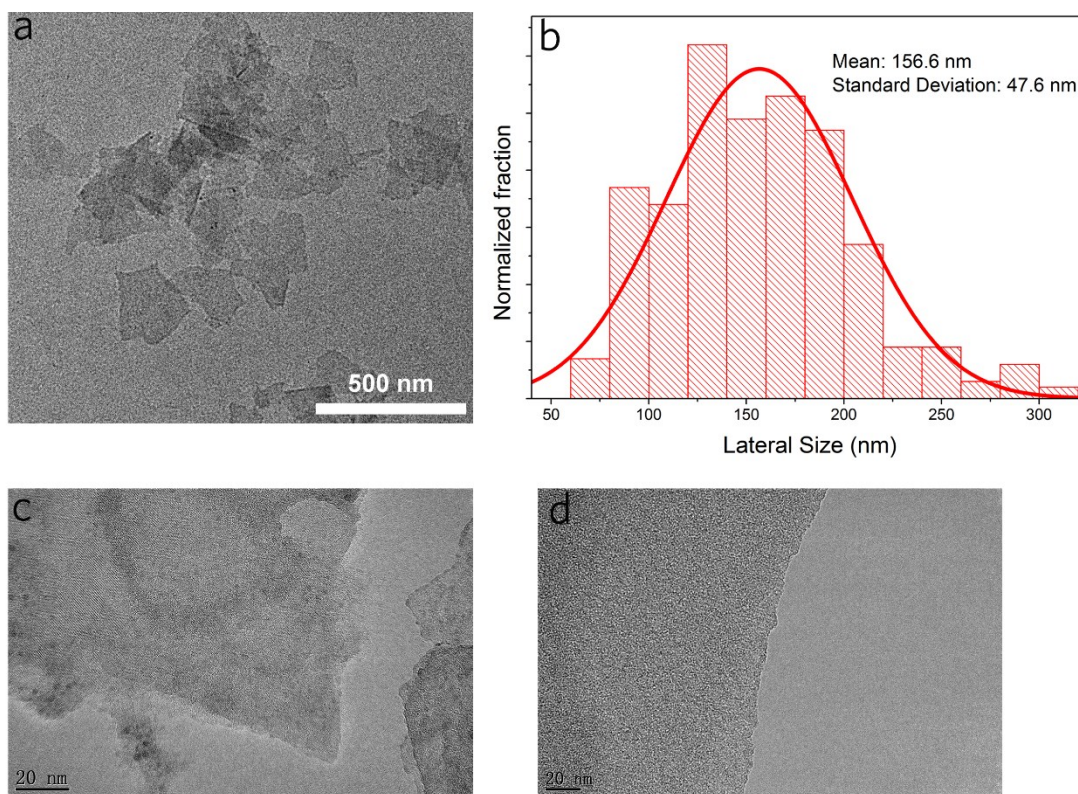
<sup>1</sup>Key Laboratory of Textile Science & Technology (Donghua University), Ministry of Education, Shanghai 201620, PR China

<sup>2</sup>College of Textiles, Donghua University, Shanghai 201620, PR China

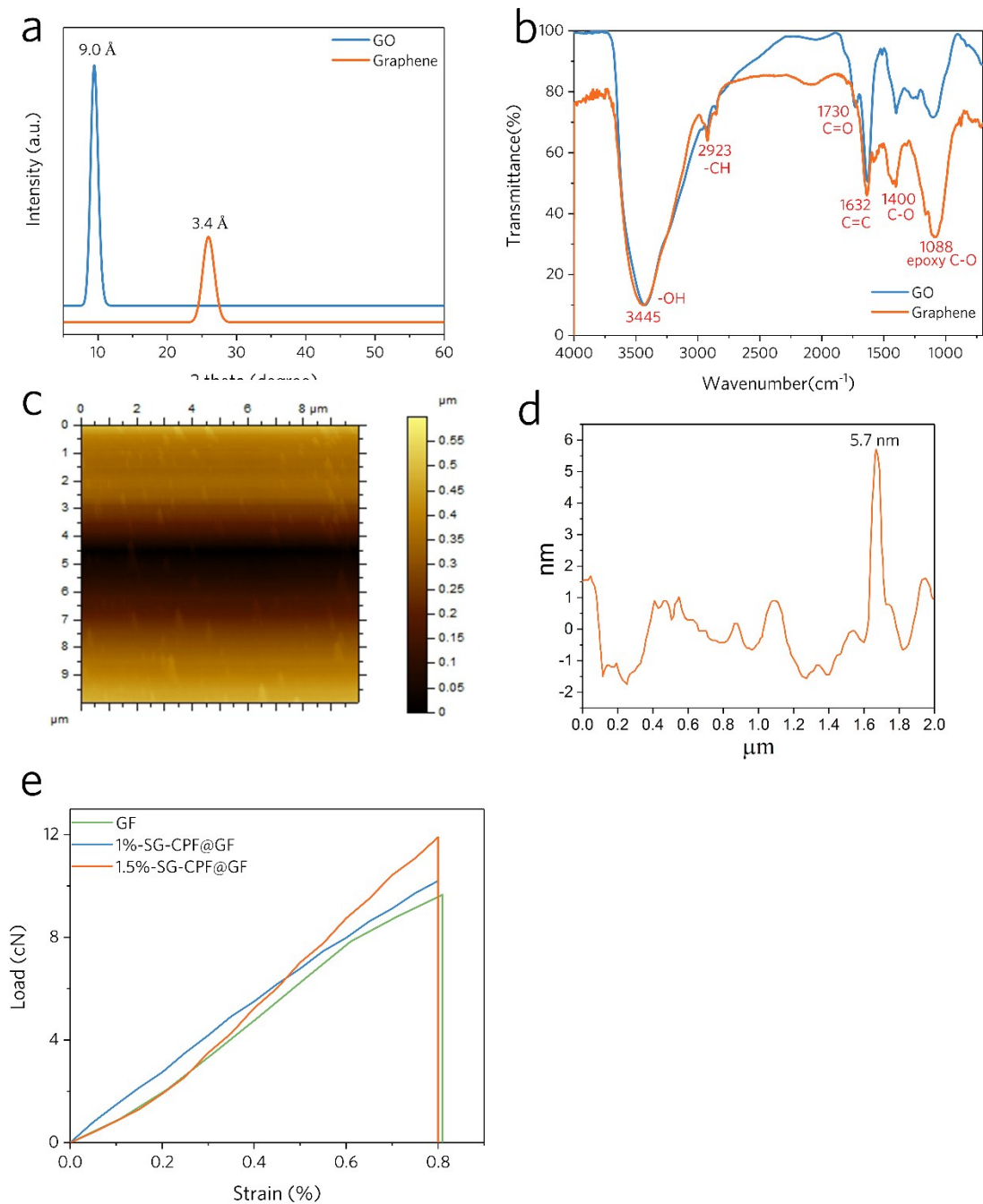
<sup>3</sup>College of Textiles and Apparel, Quanzhou Normal University, Fujian 362000, PR China

<sup>4</sup>Department of Industrial and Systems Engineering, Texas A&M University, College Station, TX 77843, United States

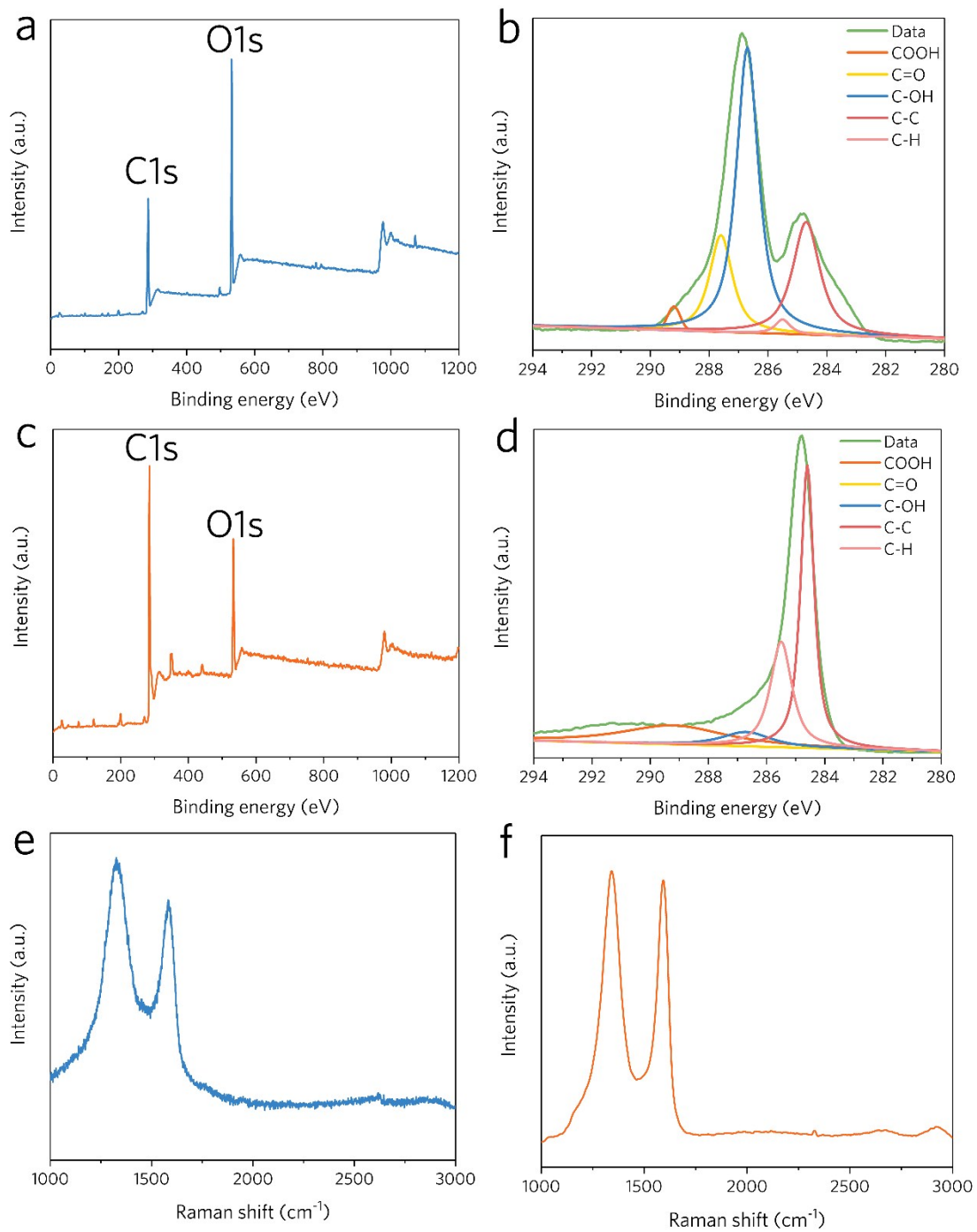
\*Corresponding author. E-mail: kun.zhang@dhu.edu.cn



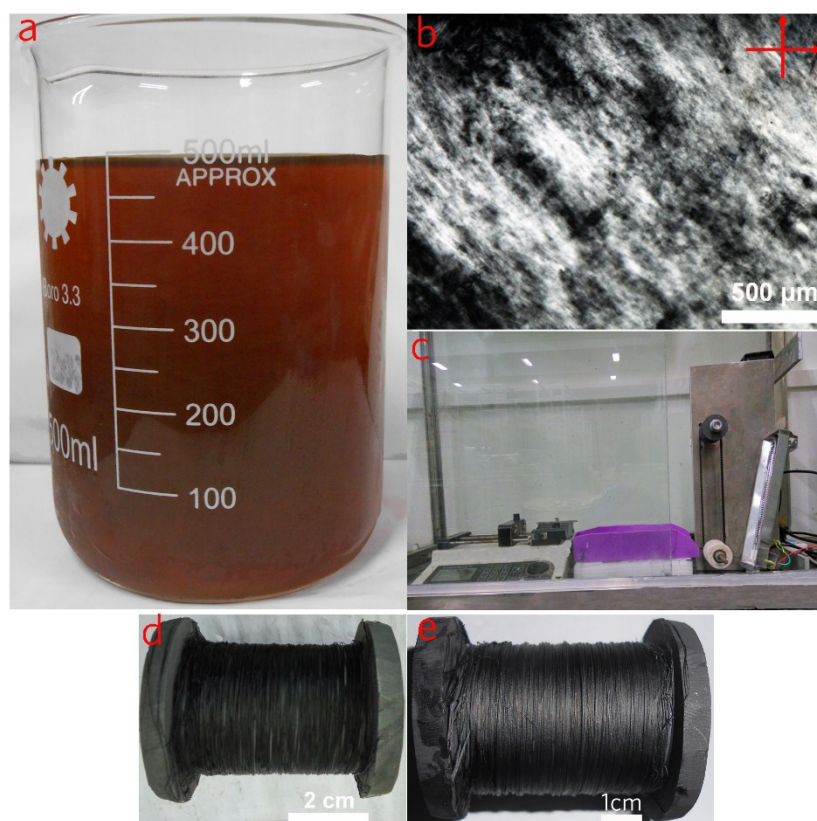
**Figure S1.** (a) TEM image of monolayer SGO sheets. (b) The corresponding lateral size distribution of SGO sheets (the diameter of an equal-area circle). High-resolution transmission electron microscopy (HRTEM) image of GO sheet (c) and graphene (d).



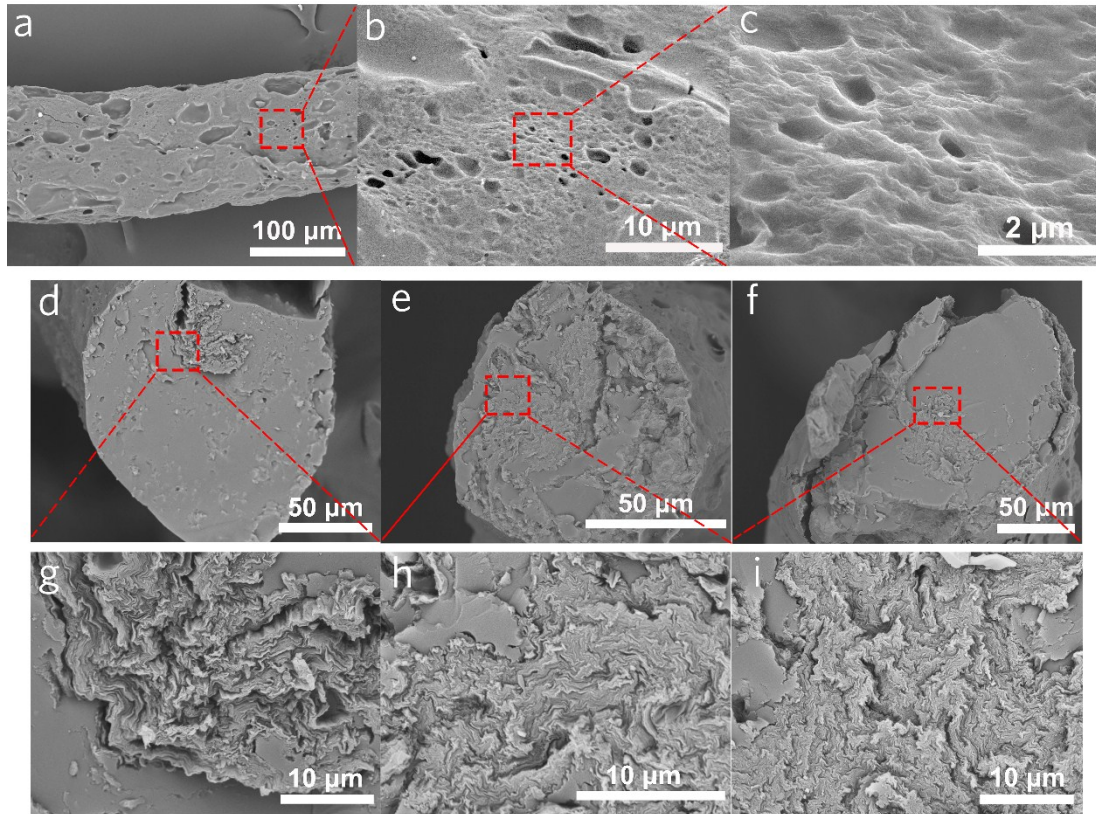
**Figure S2.** (a) XRD patterns of GO and graphene. (b) FTIR spectrum of GO and graphene. (c) AFM image of the prepared graphene (d) The corresponding height profile derived from the marked line. (e) Typical stress-strain curve of GF, 1%-SG-CPF@GF and 1.5%-SG-CPF@GF.



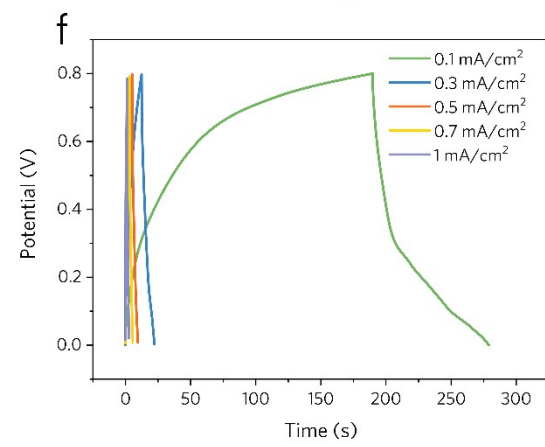
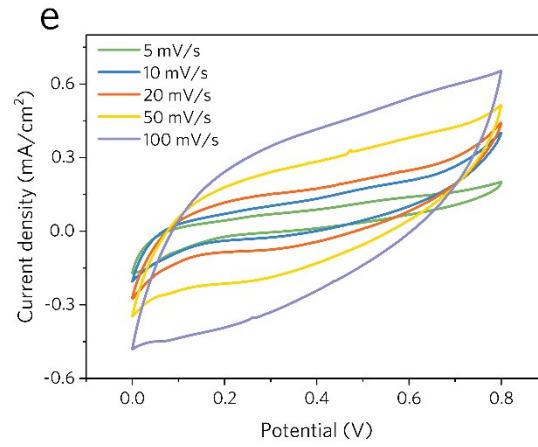
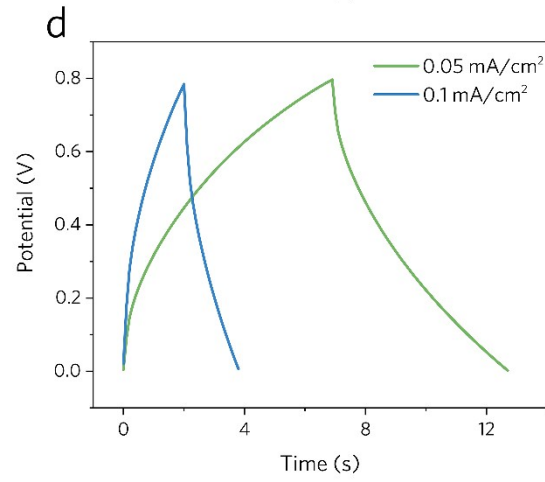
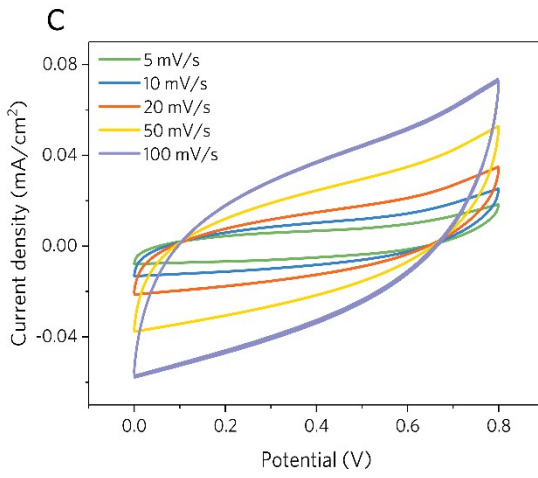
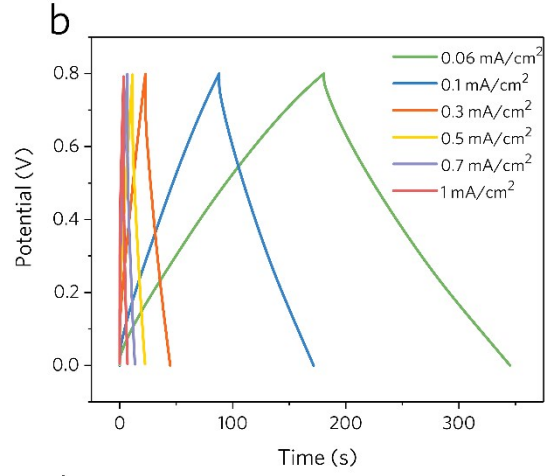
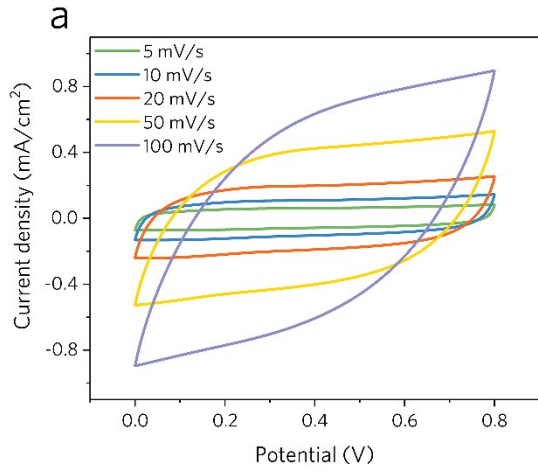
**Figure S3.** (a) The wide-scan XPS spectra of GO. (b) narrow scan XPS spectra of C1s of GO. (c) wide-scan XPS spectra of graphene. (d) narrow scan XPS spectra of C1s of graphene. The Raman spectra of (e) graphene oxide and (f) reduced graphene oxide



**Figure S4.** (a) The as-prepared large size GO. (b) Polarized optical microscopy image of large size GO spinning dope. (c) The home-made wet spinning machine for fabricating GOFs. (d) The as-spun continuous GOFs winded onto a graphite reel with inner diameter of 3cm. (e) GFs winded onto a graphite reel with inner diameter of 3cm.



**Figure S5** SEM images of longitudinal and transverse section of composite fibers. (a)-(c) longitudinal section of 1%-SG-PF@GF. (d)-(i) transverse section of the composite fibers: (d), (g) 0.5%-SG-PF@GF. (e), (h) 1%-SG-PF@GF. (f), (i) 2%-SG-PF@GF.



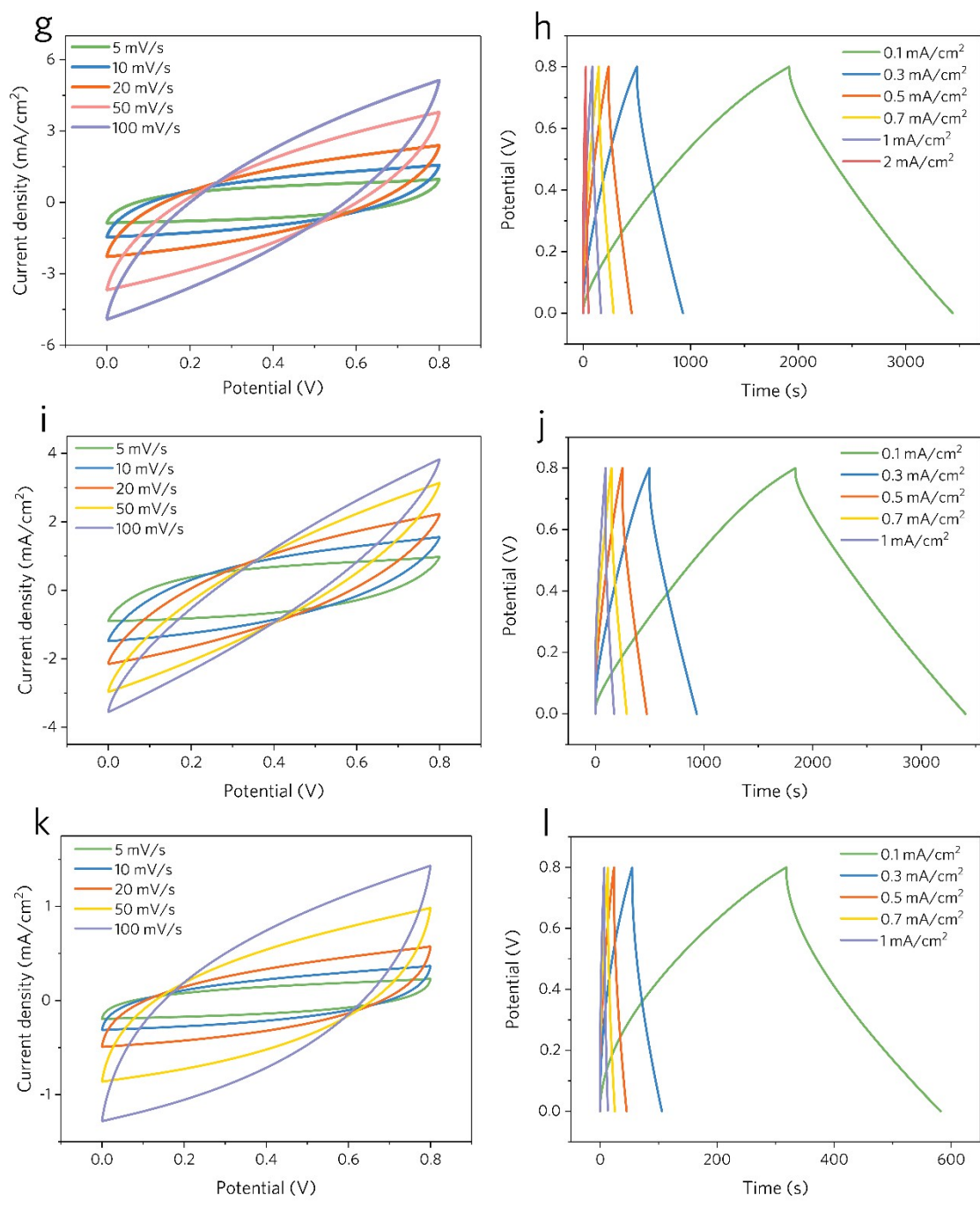


**Figure S6.** CV and GCD curves of fiber-shaped supercapacitors tested in 2-electrode cell in 1M H<sub>2</sub>SO<sub>4</sub>/PVA gel electrode. (a)-(b) GF. (c)-(d) PF@GF. (e)-(f) 0.5%-SG-PF@GF. (g)-(h) 1%-SG-PF@GF. (i)-(j) 1.5%-SG-PF@GF. (k)-(l) 2%-SG-PF@GF.

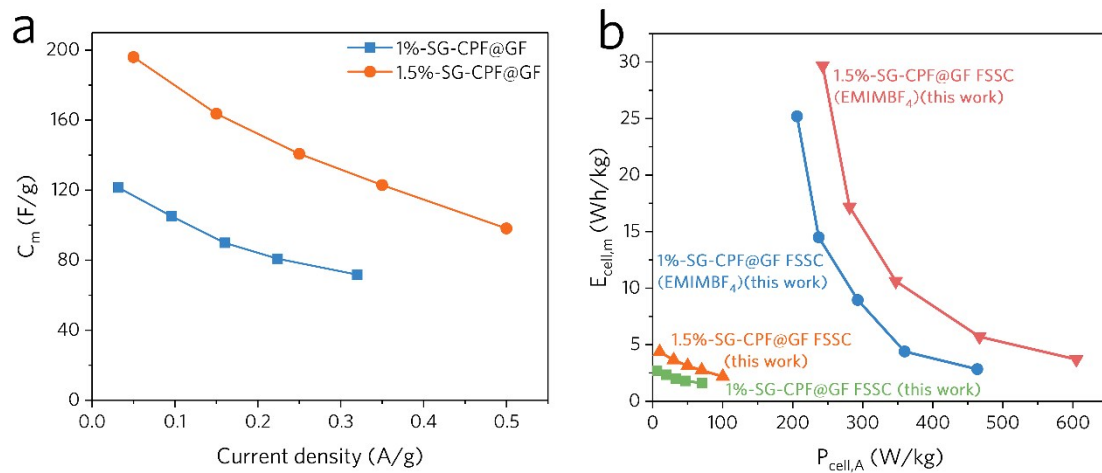


**Figure S7.** (a) Gravimetric specific capacitance ( $C_m$ ) of 1%-SG-CPF@GF and 1.5%-SG-CPF@GF at different current densities obtained from the GCD test. (b) Ragone plot of the 1%-SG-CPF@GF and 1.5%-SG-CPF@GF FSSC tested in aqueous phase and organic phase.

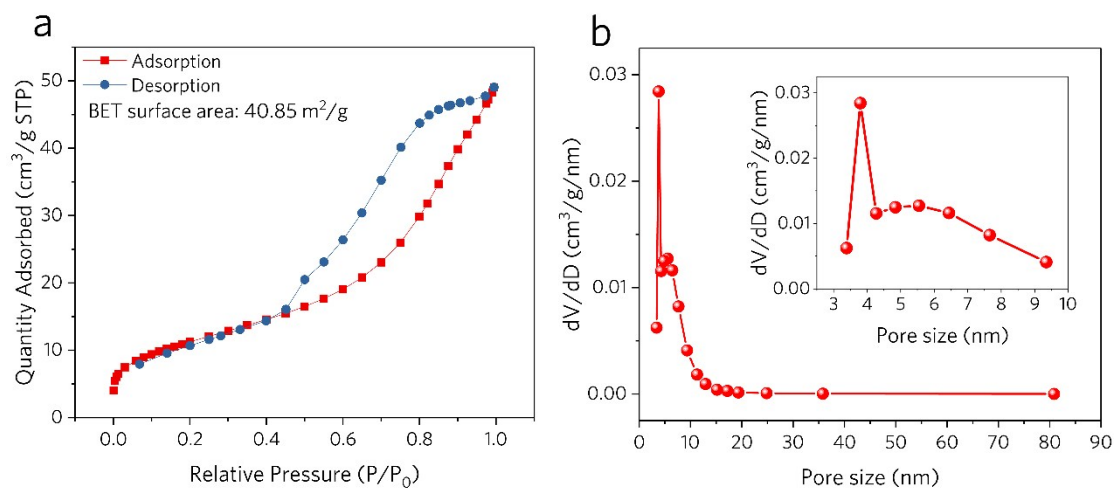


**Figure S8.**  $N_2$  adsorption/desorption isotherms of GF (a) and corresponding pore size distribution.

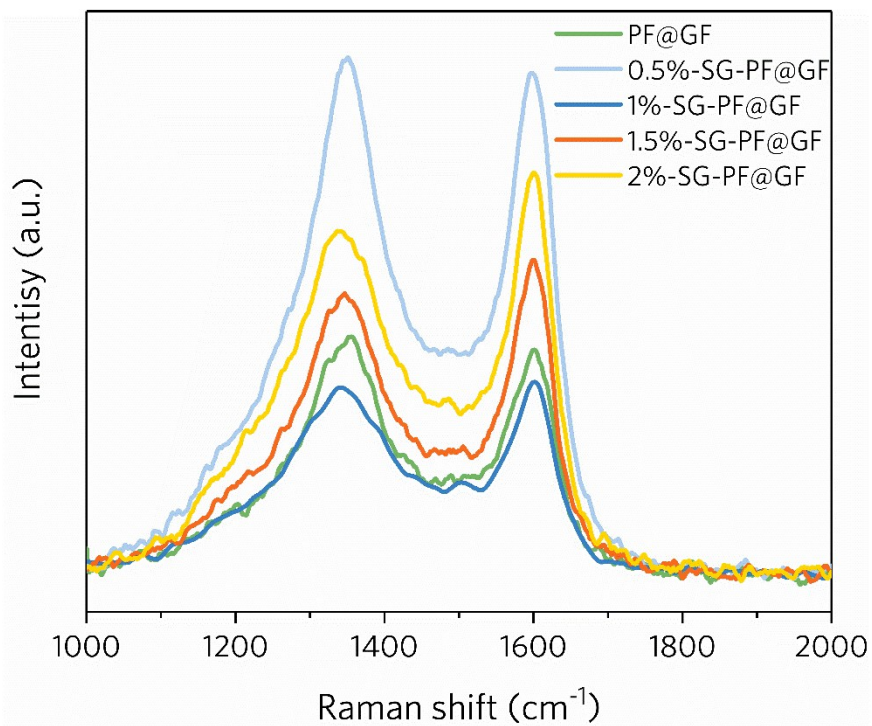


**Figure S9** Raman spectrum of as-prepared composite fibers.

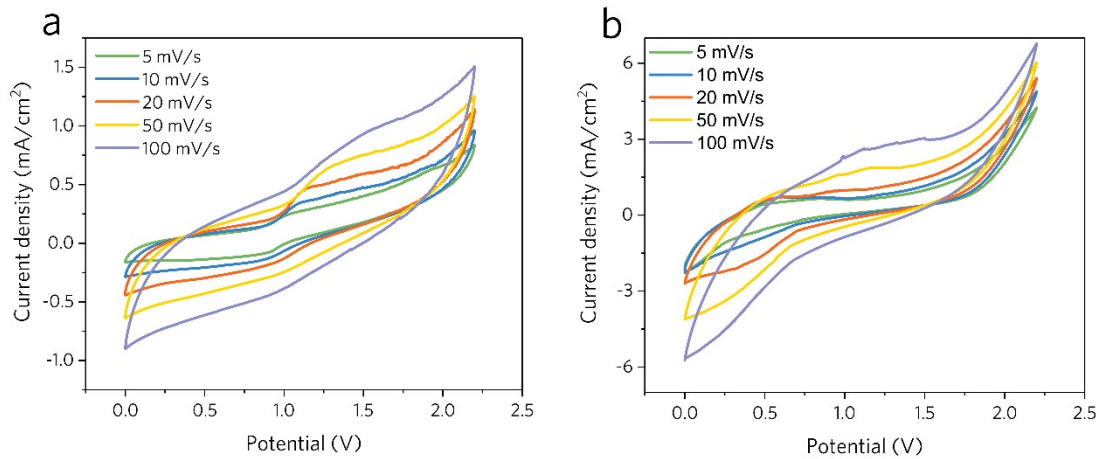


**Figure S10** CV curves composite fiber supercapacitors tested in 2-electrode cell in 1M EMIMBF<sub>4</sub>/PVDF/DMF gel electrolyte: (a) 1%-SG-PF@GF. (b) 1.5%-SG-PF@GF.

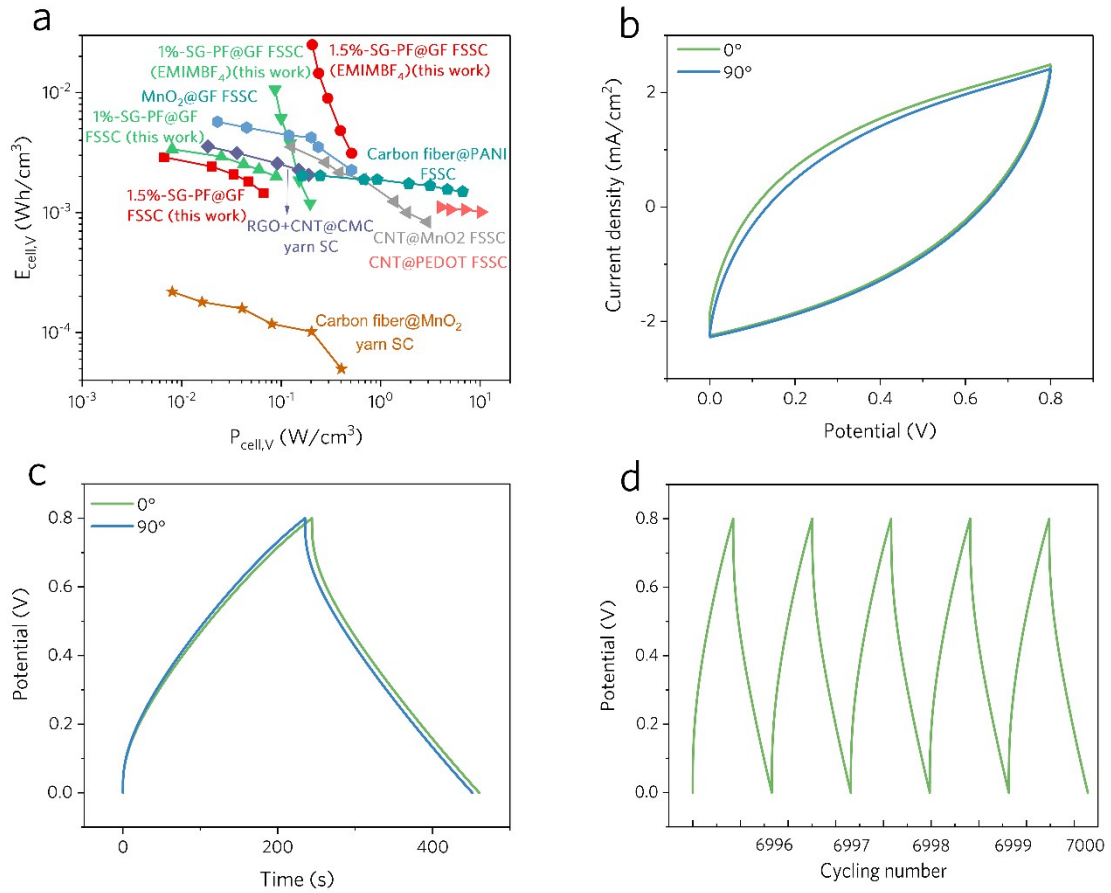


**Figure S11** (a) Volumetric Ragone plots based on the entire fiber supercapacitors to compare the SG-CPF@GF fiber supercapacitors with previously reported devices. (b) CV curves of the SG-CPF@GF fiber supercapacitors under straight and bended with  $90^\circ$  at scan rate of 20 mV/s. (c) GCD curves of SG-CPF@GF fiber supercapacitors under straight and bended with  $90^\circ$  at current density of 0.5 mA/cm<sup>2</sup>. (d) GCD curves of SG-CPF@GF fiber supercapacitors at cycle number from 6996 to 7000.